A TOF-PET prototype with position sensitive PMT readout*

CHEN Jin-Da(陈金达)[1,2;1)] XU Hu-Shan(徐瑚珊)[1] HU Zheng-Guo(胡正国)[1]
CHEN Ruo-Fu(陈若富)[1] TANG Bin(唐彬)[1,2] YUE Ke(岳珂)[1,2] YU Yu-Hong(余玉洪)[1]
ZHANG Xue-Heng(章学恒)[1] KONG Jie(孔洁)[1,2] ZANG Yong-Dong(臧永东)[1,2]
WANG Jian-Song(王建松)[1] SUN Zhi-Yu(孙志宇)[1] GUO Zhong-Yan(郭忠言)[1]

[1] Institute of Modern Physics, Chinese Academy of Sciences, Lanzhou 730000, China
[2] Graduate University of Chinese Academy of Sciences, Beijing 100049, China

Abstract: A prototype of time-of-flight positron emission computed tomography (TOF-PET) has been developed for acquiring the coincident detection of 511 keV γ-rays produced from positron annihilation. It consists of two 80.5 mm×80.5 mm LYSO scintillator arrays (composed of 35 ×35 pixel finger crystals) with the position sensitive photomultiplier tubes R2487 as the readout. Each array is composed of 2 mm ×2 mm×15 mm finger crystals and the average pixel pitch is 2.30 mm. The measured results indicate that the TOF information has the potential to significantly enhance the image quality by improving the noise variance in the image reconstruction. The best spatial resolution (FWHM) of the prototype for the pairs of 511 keV γ-rays is 1.98 mm and 2.16 mm in the x and y directions, respectively, which are smaller than the average pixel pitch of 2.30 mm.

Key words: LYSO, TOF-PET, spatial resolution, signal-to-noise ratio, coincident time resolution

PACS: 78.70.Bj **DOI:** 10.1088/1674-1137/35/1/013

1 Introduction

It has long been realized that the signal-to-noise ratio (SNR) in positron emission tomography (PET) images can be improved by incorporating time-of-flight (TOF) information [1], especially with the development of the lutetium orthosilicate [2, 3] scintillator and the lutetium yttrium orthosilicate (LYSO) [4] scintillator, which have a high light yield, short decay time, high effective atomic number and photoelectric fraction. TOF-PET has become a popular topic in recent years.

The TOF-PET technique can be classified into two major types according to the signal readout. One adapts the Anger logic technique and the other uses the position sensitive photomultiplier tubes (PS-PMTs) [5] and position-sensitive avalanche photodiodes [6]. The Anger logic technique also has two types: the conventional technique with light guides [7, 8] and the photomultipliers in quadrant sharing configuration (PQS) technique without light guides [9].

For high resolution and low cost detectors, PS-PMTs are good candidates as sensors [10]. And the TOF information is extracted from the PS-PMT R2487, which greatly improves the SNR in image reconstruction.

It would be useful to study the optimum design of the TOF-PET prototype by better understanding the factors influencing the image quality. Therefore, some factors affecting the imaging performance have being studied in our experiments, including the influence of the shapes and materials of light guides, the model of the trigger signal, the types of constant fraction discriminators and timing amplifiers, the shaping delay time of the discriminator and so on.

The experimental results indicate that the TOF information greatly enhances the image quality by improving the noise variance in the image reconstruction. The light guide has an important influence on

Received 26 March 2010

∗ Supported by National Natural Science Foundation of China (10305015,10475098), West Light Foundation of Chinese Academy of Sciences(0801010XBB) and Major Foundation Program of Chinese Academy of Sciences(O701050YZD)

1) E-mail: chenjinda@impcas.ac.cn

the spatial resolution, and the shaping delay of the constant fraction discriminator and the types of timing amplifier also affect significantly the timing resolution.

2 The prototype detector and test electronics

The prototype detector consists of two 80.5 mm× 80.5 mm LYSO scintillator matrices coupled to the PS-PMTs R2487. In the experiments, some optical couplings were studied. One is the LYSO crystal array coupled to PS-PMTs R2487 by optical grease without light guides; and the other is the crystal array coupled through the Bicron optical grease with different types of light guides (as shown in Fig. 1(b), (c), (d)).

2.1 The scintillator array

As illustrated in Fig. 1(a), each LYSO array is made up of 35×35 finger crystals with the dimensions 2 mm×2 mm×15 mm, and the average pixel pitch is 2.3 mm. Each finger crystal was wrapped with $BaSO_4$ tape, and all 1225 crystals were encapsulated with Teflon tape to form an array. The PS-PMT and the LYSO array were sealed in a duralumin housing for mechanical support and light shielding.

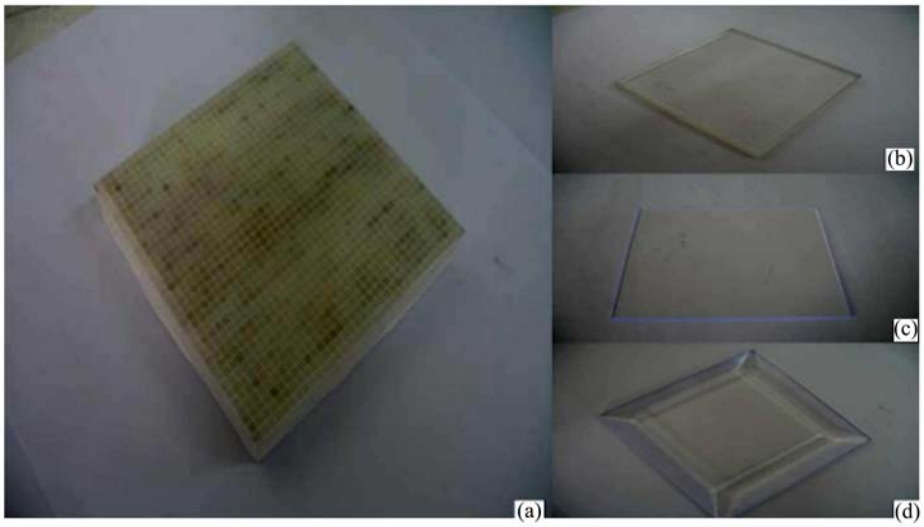

Fig. 1. The profile of the LYSO crystal array and various light guides: (a) the LYSO array with dimensions 80.5 mm×80.5 mm×15 mm, (b) the poly glass light guide type B with dimensions 80.5 mm×80.5 mm×5 mm, (c) the plastic scintillator light guide type C with dimensions 80.5 mm×80.5 mm×1 mm, (d) the plastic scintillator light guide type D with dimensions 80.5 mm×80.5 mm×10 mm, the dimensions of the small square are 55 mm×55 mm.

The LYSO scintillator is produced by Shanghai Institute of Ceramics, the Chinese Academy of Sciences. The LYSO scintillator has relatively high light output (about 26000 photons/MeV) and short scintillation decay time (41 ns), which indicate that it should have excellent timing resolution.

2.2 The PS-PMT

The PS-PMT R2487 has a bialkali photocathode, a 12-stage coarse mesh dynode structure (as shown in Fig. 2(a)), and multiple anode wires crossing one another in the x and y directions. As shown in Fig. 2(b), the output signals from each anode are divided through external resistive chains and derived from x and y electrodes as the position signals.

In most cases, obtaining 2-dimensional information requires the use of an arrangement of multiple PMTs, which is costly and requires complex hardware.

The R2487 is a position sensitive PMT. Therefore, it is possible to reduce the cost for the TOF-PET prototype by using an R2487. For the purpose of reaching the optimum performance of the system, we successfully extract the timing signals [11] from the 10th dynode of the PS-PMT (as shown in Fig. 2(a)), which make sit possible to acquire the TOF information.

2.3 Test electronics

To test the performance of the prototype detector, some coincidence measurements have been carried out. The scheme of the coincidence electronics and data acquisition is illustrated in Fig. 3.

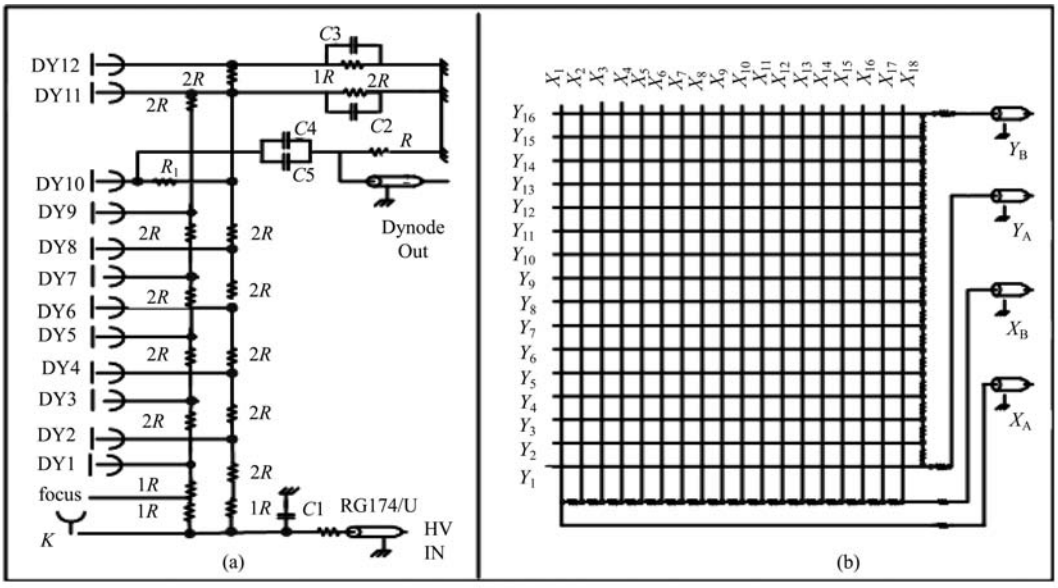

Fig. 2. (a) Schematic diagram of the voltage divider. The signal is introduced from the 10th dynode. (b) The multiple anode wires and the position signal output.

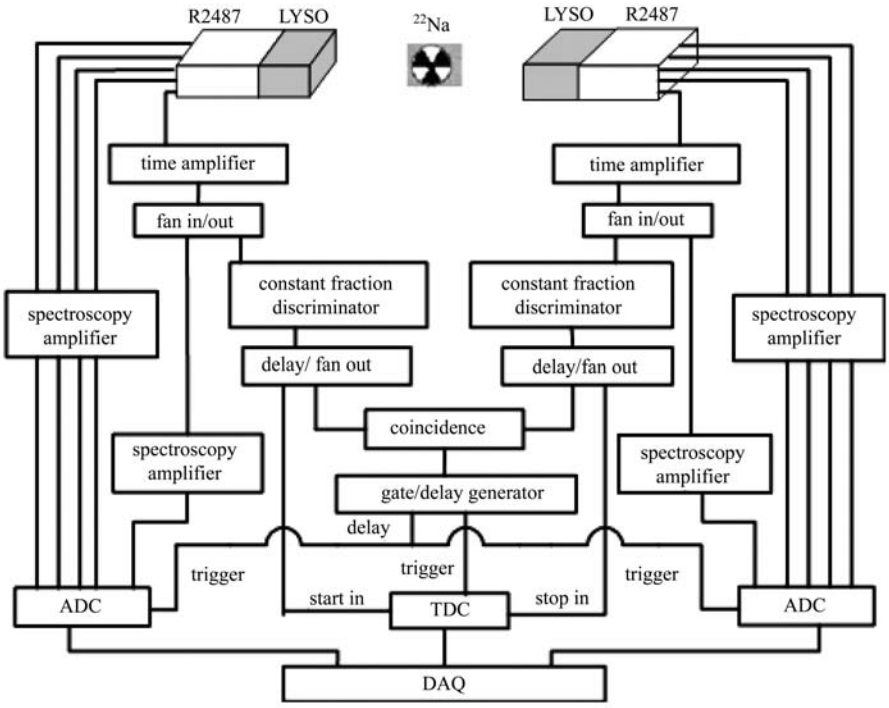

Fig. 3. The scheme of the coincidence electronics and data acquisition for the prototype.

3 Test results

In order to obtain the optimum design for the TOF-PET prototype, the factors affecting the system imaging performance have been studied, including the effects of light guides, the electronic instrument modules, the models of the trigger signal and so on. The details of the influence on image properties and optimum experimental results are given in the following.

3.1 Spatial resolution of the prototype detectors

In this paper, two detectors consisting of two LYSO scintillator arrays coupled to the PS-PMTs R2487 were used. A 4.16 μCi ^{22}Na plane source was placed between the two detectors. The high voltage for the first detector was set at −1190V, and the second was kept at −1040 V.

The optimum measured results of the coincidence

time resolution and spatial resolution were shown in Fig. 4. The original time spectrum of the pairs of annihilation events measured by the crystal array is illustrated in Fig. 4(a). Fig. 4 (b) and (c) show one dimensional profiles of the crystal decode map for the start detector in the x and y direction, respectively. The optimum crystal array time resolution is 1321 ps, from which the electronic system time resolution of 348 ps has been subtracted. The average spatial resolution (FWHM) of the start detector is 1.98 mm in x direction and 2.16 mm in y direction. They are all smaller than the actual average detector pixel pitch (2.30 mm), which means that the capability of the spatial discrimination is good enough.

3.2 Effects of the light guide

In order to understand the influence of light guide shape on the spatial resolution, the comparisons among the measured results for the three types of light guide as shown in Fig. 1 were performed.

The one-dimensional profiles of the decoding map for the LYSO array in the x direction with different types of light guide are illustrated in Fig. 5. The average spatial resolution (FWHM) is 2.02 mm without a light guide (a), 2.88 mm with a light guide of Type B (b), 2.33 mm with Type C (c) and 4.18 mm with Type D (d).

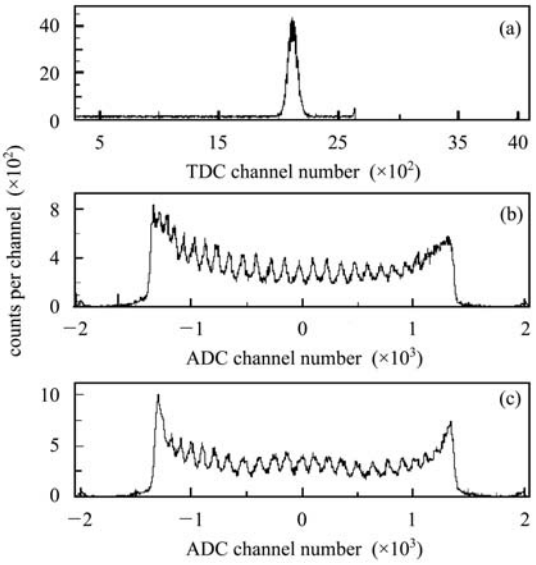

Fig. 4. The time coincidence spectra of the pairs of annihilation events and profile of the crystal decode map: (a) time spectrum, (b) the x direction decode map, (c) the y direction decode map.

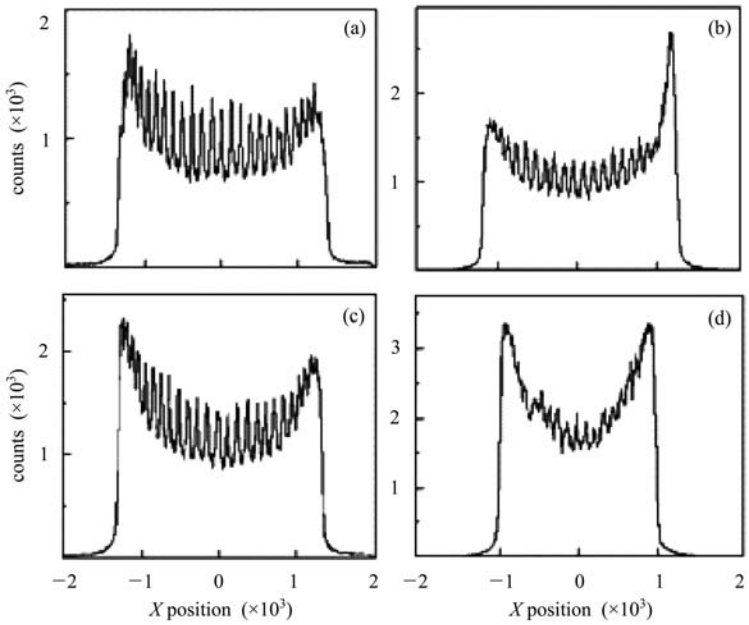

Fig. 5. One-dimensional profile of the crystal decoding map in LYSO arrays coupled with different types of light guides: (a) without light guide, (b) Type B, (c) Type C and (d) Type D.

From the results of the comparisons, one can see that the light guide shape has an important influence on the spatial resolution. This is mainly caused by the transmission of the scintillation light in the light guide.

3.3 Effects of the electronics

In our measurements, different kinds of NIM modules were used to reach the best resolution of the prototype system. The detectors were made up of the LYSO arrays coupled to PS-PMTs R2487. The trig-

ger signals were from the dynode.

The measurements of properties of the prototype were carried out by using the constant fraction discriminator (CFD) CF8000 with various settings for shaping delay and keeping other conditions fixed. The results are presented in Table 1. While the shaping delay time is 10 ns, the time resolution is the best. Therefore, the shaping delay is an important factor affecting the time resolution. The influence may be explained by the following empirical formula for the best timing performance of CFD,

$$t_{\rm delay} = t_{\rm rise} \cdot (1 - f), \quad (1)$$

where $t_{\rm delay}$is the selected shaping delay on CFD, $t_{\rm rise}$ is the rise time of the input signal and f is the constant fraction value of CFD.

In the comparing measurements, the detectors and the model of trigger signals were fixed. However, the timing amplifiers and discriminators were not the same in each experiment. The results and types of the electronic modules are shown in Table 2. It is found that the types of timing amplifier and constant discriminator have a significant effect on the time resolution. The resolution of FTA 810 is much better than that of TA474. The reason is possibly a higher gain of FTA810 than TA474. The time resolution with CF715 is the best. The resolution with CF8000 is similar to that with CF715. A large deterioration in the resolution with CF583 plus TA474 occurred. This may be caused by setting the threshold of CFD to a lower one. However, the types of timing amplifier and discriminator influence the spatial and energy resolution very little.

Table 1. The resolutions depend on the shaping delay (SD) time of CF8000.

SD time/ns	time resolution/ns	x-spatial resolution (FWHM)/mm	y-spatial resolution (FWHM)/mm	energy resolution (%)
2	4.28	2.16	2.22	31.1
4	2.79	2.12	2.24	32.4
6	1.73	2.21	2.40	28.2
8	1.55	2.20	2.32	28.8
10	1.26	2.25	2.25	33.2

Table 2. The effects of various CFD and Timing Amplifier (TA) on the resolutions.

CFD (SD=10 ns)	TA	differential /ns	time resolution/ns	x-spatial resolution (FWHM)/mm	y-spatial resolution (FWHM)/mm	energy resolution (%)
CF8000	TA 474	20	1.52	2.06	2.16	35.0
	FTA 810	–	1.26	2.25	2.25	33.2
CF583	TA 474	20	4.78	2.17	2.48	31.4
	FTA 810	–	1.90	2.13	2.25	31.8
CF715	TA 474	20	1.32	1.98	2.16	34.2
	FTA 810	–	1.19	2.3	2.08	33.5

3.4 The advantage of using TOF information

To improve the SNR in the image reconstruction by incorporating TOF information, we extract the TOF information from the PS-PMT R2487. The design of the voltage divider is illustrated in Fig. 2(a). We compared the reconstruction image with and without TOF information, as shown in Fig. 6. From the comparison, it is obvious that the SNR of the position decoding map is greatly increased by incorporating the TOF information. And the coincidence time resolution is only 1.32 ns.

The same results were proved by other groups doing research on TOF-PET. For example, with 1.26 ns coincidence time resolution, Watson [12] has shown an increase by 55%–116% in clinical image noise variance based on the measured data from a Simens Biograoh Hi-Rez PET/CT. Similarly, Conti [13] has shown experimentally and in simulations a 50% increases in SNR in reconstructed images of phantoms about 40 cm in diameter with 1.2 ns time resolution.

Therefore, the design of extracting the signal from the dynode of the PS-PMTs, which makes it possible to obtain the TOF information, is successful. It proves that the TOF information has the potential to significantly enhance the image quality by improving the noise variance in the image reconstruction.

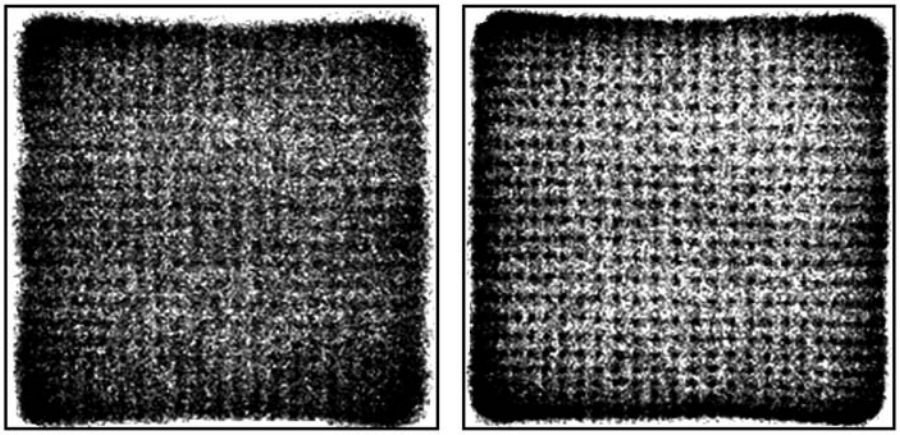

Fig. 6. 2-D crystal position decoding map of 35×35 LYSO arrays. The left picture represents the flood map triggered by the anode signal. The right picture is the flood map triggered by the dynode signal.

4 Conclusions

The signal from the dynode of the PS-PMT R2487 is successfully extracted, which makes it possible to measure the TOF information. The measured results indicate that the TOF information has the potential to significantly enhance the image quality by improving the noise variance in the reconstruction.

The light guide is an important factor affecting the image quality. At the same time, several different types of constant fraction discriminators and time amplifiers have been compared in terms of the imaging performance. The shaping delay time of the discriminator is also investigated in the experiments. It is found that the shaping delay time is a significant factor affecting the time resolution, but not the key factor, and the types of the constant fraction discriminator and timing amplifier are also important to improve the time resolution for our prototype system.

Therefore, these results would be useful to research the optimum design of the TOF-PET prototype in the future.

References

1 LIU Ji-Guo, LIU Shi-Tao et al. IEEE NSS Conf. Rec., 2007, **8**(2): 3294
2 Casey M E et al. IEEE Trans. Nucl. Sci., 1997, **44**(3): 1109–1113
3 Moszynsky M et al. Nucl. Instrum. Methods A, 1996, **372**(1); 51–58
4 Pepin C M et al. IEEE NSS Conf. Rec., 2002, **2**: 655–660
5 Moriya T et al. IEEE NSS Conf. Rec., 2007, **4**: 2842–2846
6 WU Y et al. IEEE Tran. NUcl. Sci. 2008, **55**(1): 463–468
7 Mechmet Aykac et al. IEEE Tran. NUcl. Sci., 2006, **53**(3): 1084–1089
8 Moszyński M et al. IEEE Tran. NUcl. Sci., 2006, **53**(5): 2484–2488
9 LIU Ji-Guo et al. IEEE NSS Conf. Rec., 2007, **5**(3): 3294–3304
10 Kitamura K et al. IEEE Tran. NUcl. Sci., 2002, **49**(5): 2218–2222
11 Jinda Chen et al. Submitted for publication
12 Watson C. IEEE NSS Conf.Rec., 2005, **4**: 2041–2045
13 Conti M et al. Phys. Med. Biol., 2007, **50**(8): 4507–452